

## Numerical simulation of soot formation in a laminar axisymmetric diffusion propane flame

Simulación numérica de la producción de hollín en una llama laminar de difusión axisimétrica de propano

MSc. Adalberto Salazar Navarro

<sup>1</sup>Universidad Técnica Federico Santa María, Valparaíso Chile, Orcid: <https://orcid.org/0000-0001-5257-3175>, email: [adalberto.salazar@sansano.usm.cl](mailto:adalberto.salazar@sansano.usm.cl)

Cómo citar: A. Salazar-Navarro, "Simulación numérica de la producción de hollín en una llama laminar de difusión axisimétrica de propano", *Rev. Ingenio*, vol.20, n°1, pp. 46-52, 2023, doi: <https://doi.org/10.22463/2011642X.3589>

Received date: jun 26, 2022  
Approved date: december 16, 2022

### ABSTRACT

#### Keywords:

Flame height, SDS,  
Soot formation, Flame  
temperature

In this work, a computational study of soot formation for a propane flame is carried out. These simulations were carried out considering the effect of using parameters such as flow velocity and mass flow per unit area to predict soot formation. Parameters such as flame height and temperature are also taken into account. In this paper, the Fire Dynamics Simulator (FDS) computational tool is used to observe the behavior of soot formation in a laminar propane (C<sub>3</sub>H<sub>8</sub>) diffusion flame. In particular, the results of this software are compared with (a) experimental data presented in the literature and (b) with the Large Eddy Simulation (LES) and Direct Numerical Simulation (DNS) approaches, which are used to predict parameters such as soot formation, flame height and flame temperature reached. The results obtained show a good performance compared to the experimental results.

### RESUMEN

#### Palabras clave:

Altura de llama, FDS,  
Formación de hollín,  
Temperatura de llama

En este trabajo se realiza el estudio computacional de la formación de hollín para una llama de propano. Estas simulaciones, se realizaron teniendo en cuenta el efecto del uso de parámetros como, la velocidad del flujo y el flujo masico por unidad de área, para la predicción de la formación de hollín. También se tienen en cuenta parámetros como la altura de llama y la temperatura. En el presente artículo se utiliza la herramienta computacional Fire Dynamics Simulator (FDS) para observar el comportamiento de la producción de hollín en una llama laminar de difusión de propano (C<sub>3</sub>H<sub>8</sub>). En particular, se comparan los resultados de este software con (a) datos experimentales presentados dentro de la literatura y (b) con las aproximaciones Large Eddy Simulation (LES) y Direct Numerical Simulation (DNS), las cuales se emplean para predecir parámetros como, la producción de hollín, altura de llama y la temperatura de llama alcanzada. Los resultados obtenidos muestran un buen comportamiento frente a los resultados experimentales.

### 1. Introduction

The formation of particulate matter resulting from combustion in various thermodynamic internal combustion reactors is known as soot. This is a topic of great interest to combustion engineers and researchers because a significant portion of this soot is composed of carbon, which can have significant environmental and health impacts [1]. Strict standards have been implemented worldwide for controlling pollutant emissions. This has piqued the interest of professionals in the combustion field and opened up possibilities for developing new and improved techniques for controlling soot production in combustion processes [2-4].

To achieve this goal, it is necessary to implement various models capable of predicting the combustion behavior of

different fuels, including the ability to predict soot formation with excellent approximations [5-7]. A variety of models developed for this purpose can be found in the literature [6-8]. Accurate prediction of soot formation is essential for compliance with emission control regulations and designing devices such as reactors and burners to enhance their thermal efficiency. Models with excellent predictive capabilities have been introduced, but it is crucial for them to be compared to experimental data documented in the literature. The objective is to simulate actual behavior, which can be accomplished by utilizing reaction mechanisms designed for the oxidation process of various fuels, coupled with specialized programs in the fluid dynamics of the process to achieve optimal results [5, 7]. The objective of this work is to

#### Corresponding Author

Email: [adalberto.salazar@sansano.usm.cl](mailto:adalberto.salazar@sansano.usm.cl) (Adalberto Salazar Navarro)



Peer review is the responsibility of the Francisco de Paula Santander Ocaña University  
Licensed Item CC BY-NC-ND (<https://creativecommons.org/licenses/by-nc-nd/4.0>)

simulate propane combustion using the Oxygen Index (OI) in the mixture to predict the behavior of soot formation and flame height. For this purpose, simulations are performed for an IO of 25% and compared with the experimental results obtained by [9] under the same IO. Section 2 elaborates on the simulation setup using the computational tool FDS (Fire Dynamics Simulator) developed by the National Institute of Standards and Technology (NIST) [10-11]. This program utilizes computational dynamics models to study heat transfer and fire smoke formation. The software solves an approximation of the Navier-Stokes equations using Large Eddy Simulation (LES) to simulate large-scale structures and model small-scale structures with approximations. Alternatively, it uses Direct Numerical Simulation (DNS) to calculate terms directly without approximations. The simulations involve a simple one-step chemical reaction, described as  $F + s(O_2 + N_2) \rightarrow (1 + s)P$ , with reactants (fuel and oxidant) and products. The program is configured to represent the volumetric concentration for the oxidant.

## 2. Methodology

### 2.1 Experimental conditions

The simulation replicates the experimental conditions described in [9]. To achieve this, a concentric tubular burner is used, consisting of an internal tube with a 10.9mm internal diameter for fuel injection and an external tube with a 100mm diameter for oxidant passage. The oxidant, a mixture of O<sub>2</sub> and N<sub>2</sub> gases, is injected separately at atmospheric pressure. To achieve varying oxygen rates, the N<sub>2</sub> flow is adjusted between 75.2 slpm and 34.1 slpm, while maintaining a constant O<sub>2</sub> flow of 20 slpm. The fuel is consistently injected into the burner at a flow rate of 1,223 cc/s, as shown in

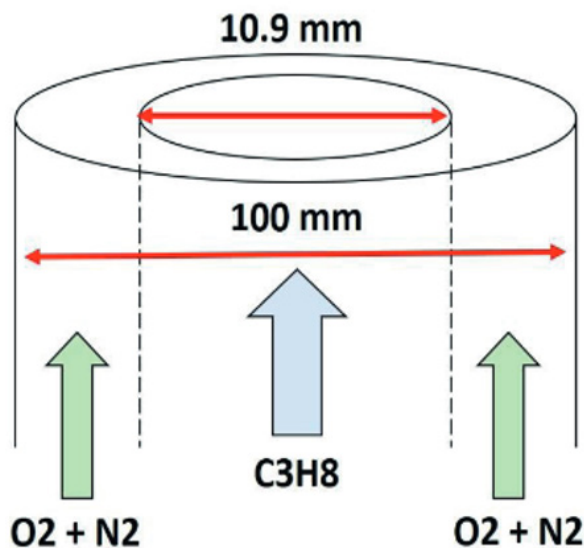


Figure 1. Burner schematic

### 2.2 Model configuration in FDS

The program uses a simplification to two dimensions in cylindrical coordinates to perform the simulations, enabling the study of the laminar behavior of a diffusion flame. Calculations are performed to determine the flow velocities for the fuel and oxidizer to configure the burner within the program. The summary of the calculations is shown in the following table.

Table 1. Flow characteristics

Especie	C <sub>3</sub> H <sub>8</sub>	O <sub>2</sub> +N <sub>2</sub>
Área de salida (m <sup>2</sup> )	9.33E-05	7.85E-03
Flujo (slpm)	0.07398	80
Velocidad (m/s)	0.013	0.202
Flujo másico por área (kg/m <sup>2</sup> s)	0.012	0.102

The simulations may produce less accurate results due to their low operating velocities, as the diffusion term tends to dominate mass transport [12]. To mitigate this issue, we decided to use the mass flow per unit area of the gases instead of velocity, as errors can arise within the simulation.

Two DNS simulations were performed to verify this behavior, one using flow velocity and the other using mass flow per unit area. The first results show that the simulation configured with the velocity does not have a stable flame behavior as shown in Figure 2.

These simulations were performed to determine flame stability. Coarse grids were used, and LES was employed to reduce computational time. Considering the above, it is possible to perform a better mesh distribution, concentrating the finer mesh in the reaction zone.

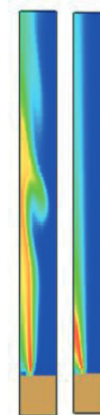


Figure 2. Comparison of flame behavior Left, using velocity. Right, using mass flow per area.

### 2.3 Code developed in FDS.

This section outlines the essential aspects of the configuration in the partially used code for the simulation. However, to maintain document brevity, it does not display the mesh configuration or obstruction locations. Two simultaneous simulations were run, one defining the flow by velocity within the code and the other by mass flow per unit area, as mentioned in the previous sections.

For simulations where velocity is defined instead of mass flow rate, the MASS\_FLUX line is replaced by VEL=-0.01310 for propane and VEL=-0.202 for the oxidizer in units of (m/s). The code allows for propane combustion, as demonstrated in Figure 2 on the right side. The surroundings are configured with 21% air.

### 2.4 Mesh construction

To enable mesh contraction, the computational domain is divided into four zones, as shown in Figure 3. These zones allow for the allocation of mesh solutions to specific processors, facilitating parallel processing. This approach enables simultaneous work on multiple meshes and the assignment of solutions to dedicated processors. Consequently, it is possible to work on meshes concurrently, optimizing computational resources by allocating more processors to the zone of interest, specifically the region where combustion occurs. This study analyzes only two meshes within Zone 1 and Zone 2, corresponding to the area where the burner is located (highlighted by the yellow box in Figure 3), due to the available computational capacity. This strategic selection aims to achieve a finer mesh resolution in the reaction zone, which reduces computation time.

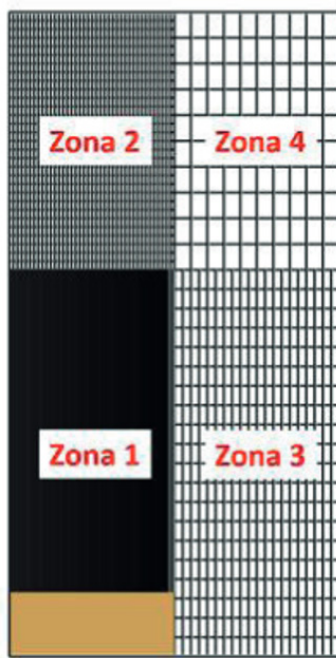


Figure 3. Grid distribution

The proposed configuration does not affect the results in Zones 3 and 4, as they only contain O<sub>2</sub> and have no direct interaction with the fuel.

Table 2. Grid configuration

Zona	Configuración de malla	Medidas (m)	
		x	z
1	100x1x100	[0-0.05]	[0-0.12]
2	100x1x50	[0-0.05]	[0.12-0.2]

### 2.5 Flame height

To determine the end of combustion in the simulation and calculate the flame height, an oxidation ratio of the mixture is used. This ratio compares the volumetric amount of oxygen and fuel to determine the reaction zone and flame boundaries. In [13], an expression is proposed to calculate the amount of oxygen and oxygen mass fraction required to burn the fuel at any point, as shown in Equation 1.

$$Ro = \frac{m_o}{m_o + \sum_c s_c m_{F,c}} \quad (1)$$

Where  $s = n_o M_o / nF M_f$ ,  $m$  is the mass fraction of oxygen,  $n$  is the number of moles and  $M$  is the molecular weight. The subscripts O and F correspond to oxygen and fuel, respectively, and the subscripts c indicate the species present in the fuel. The ratio has a value of RO=1 at the air inlet or when combustion is complete, and takes a value of RO=0 at the fuel inlet [13]. For the conditions studied in this research, the oxidation ratio for complete combustion is not defined as RO=1. Instead, the critical oxidation ratio is determined to define the flame edges within the simulation, using the following expression:

$$R_{cr} = \frac{1}{1 + \sum_j s_j \phi_j} \quad (2)$$

Where  $\phi$  represents the flammability limit of the fuel, which, in the case of propane, is determined within a range of 2.1% and 9.5% of volumetric concentration of air [14]. To find the height at which combustion is completed, equation (2) uses the lower flammability limit, which defines the flame edge. This results in a  $R_{cr}=0.126$  which defines the end of combustion and the flame edge within the simulations performed.

## 3. Results

The obtained results indicate that the flame behavior and soot formation cannot be reproduced due to the simplifications made in this study. For instance, the use of an oxidation mechanism for the 2-step fuel instead of a detailed or simplified

reaction mechanism does not explain the chemical kinetics of the reaction in a better way, which affects the prediction of the studied parameters. The code used parameters such as flow velocity and mass flow to predict the end of combustion using flame heights of  $h_{S}=0.07\text{m}$  and  $h_{s}=0.023\text{m}$  for the simulations. The results of these simulations are explained graphically in the following sections.

The simulations demonstrate the maximum soot formation under the specified conditions. However, the prediction of flame height is inaccurate. Additionally, the maximum soot formation occurs at varying radii, which is consistent across both studied cases. The comparative figures illustrate the outcomes obtained through the aforementioned parameters, including flow velocity and mass flow per unit area.

Based on the conducted analysis, a comparable temperature distribution is evident in both cases. The two simulations, employing distinct parameters for prediction, exhibit exceptional accuracy in foreseeing the maximum temperature recorded in the conducted experiments for the given oxygen percentage.

However, there is a significant difference between the predicted flame heights in each case, as shown in Figure 4. The simulations show a similar distribution for soot prediction, and both reach maximum soot formation under the two conditions studied.

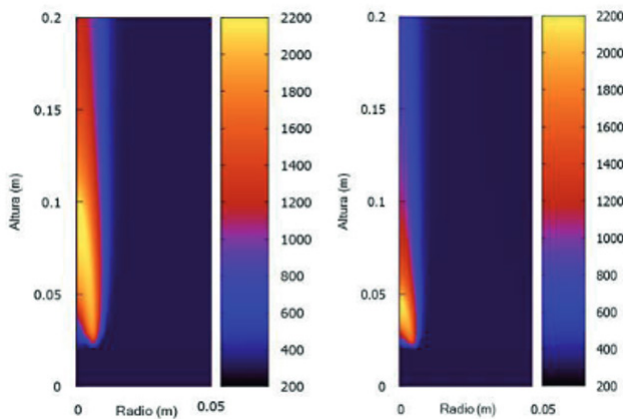


Figure 4. Difference between the use of velocity (left) and mass flow per unit area in a DNS simulation (right).

The numerical simulations do not present a maximum soot formation or production distribution in relation to burner radius, as shown in the experimental results. Figures 5, 6, 8, and 9 show the experimental results as continuous lines and the results obtained from the numerical simulations as dashed lines.

### 3.1 Simulation using discharge velocity.

This section presents the results obtained by using the discharge velocity of the mimics as a flow definition parameter for both fuel and oxidant. Figure 5 compares the experimental results obtained by [9] with the results of this study.

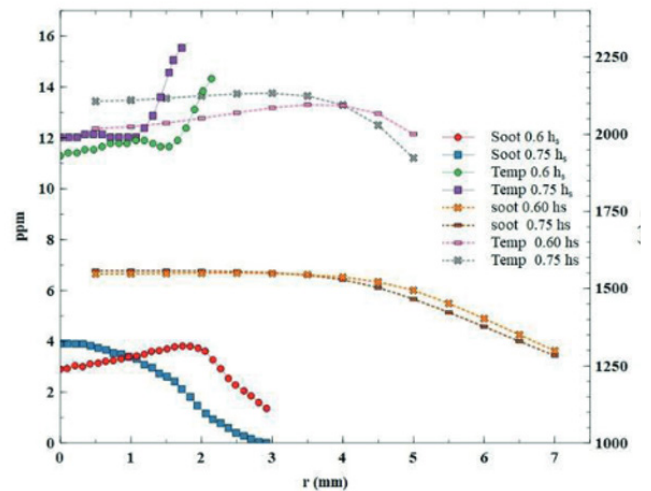


Figure 5. Comparison between numerical and experimental results.

The results show a difference in the distribution of soot production based on the burner radius when compared to the experimental data. According to the experimental findings, the highest soot formation occurs at a radius of approximately 2 mm. However, the simulations indicate that the maximum soot formation occurs at approximately 5 mm, near the fuel outlet.

Figure 6 compares the results in relation to the burner radius. It is observed that, for the same radius, the experimental results show relatively constant soot formation and temperature. In the case of the latter (see Figure 6), the simulations are close to the experimentally recorded temperatures with a difference of 156 K on average.

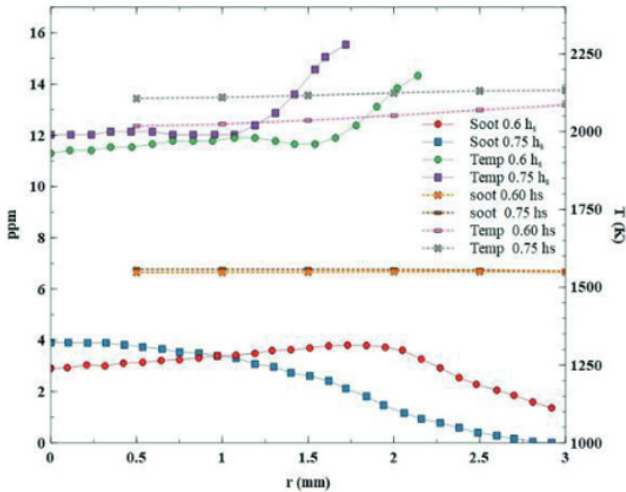


Figure 6. Comparison between numerical and experimental results for the same radius.

Finally, Figure 7 shows the distribution of soot formation in relation to the radius. This figure shows a similar behavior to that presented in the experimental results, but in this case, it occurs at different radii.

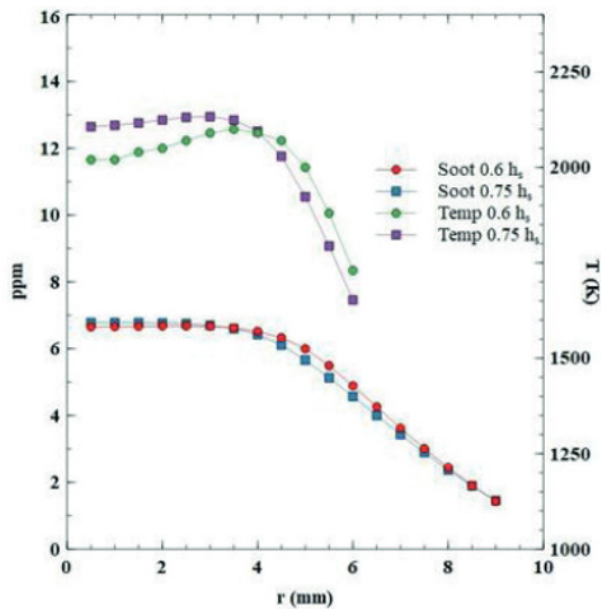


Figure 7. Soot formation and temperature

### 3.2 Simulation using mass flow per unit area

This section presents the results obtained by using mass flow per unit area as a definition parameter for the simulation of fuel and oxidant. The results obtained using this parameter are similar to those obtained using flow velocity as a parameter. The difference between the two is reflected in the flame height, which is lower for the area mass flow and results in lower temperatures. However, the same distribution as in the

previous sections can be observed. Figure 8 shows that, for the same radius compared to Figure 6, the soot formation is much lower and decreases with higher slope.

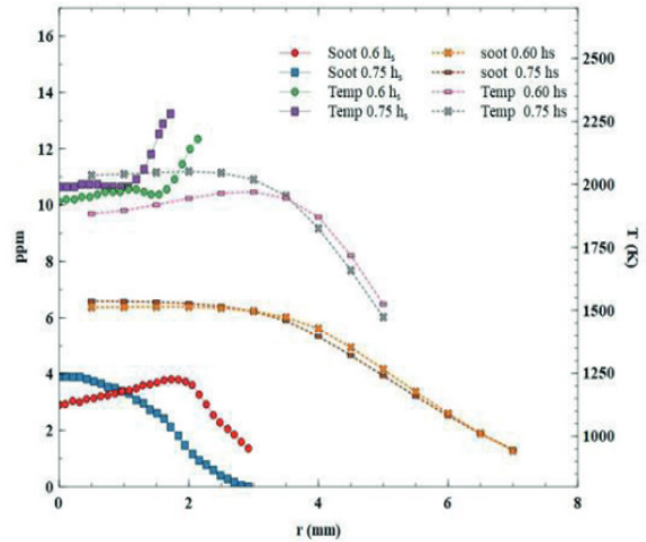


Figure 8. Comparison between numerical and experimental results.

Figure 9 shows a trend similar to the one observed in the previous case (Figure 6) for the corresponding radius in the experimental results. Soot formation and its associated temperature remain stable within the radius range of 0 to 3 mm, with only slight variations in their magnitudes.

Figure 9 shows the distribution of soot formation and temperature at a specific height. This distribution is similar to the experimental data, as shown in Figure 10, although at a different radius.

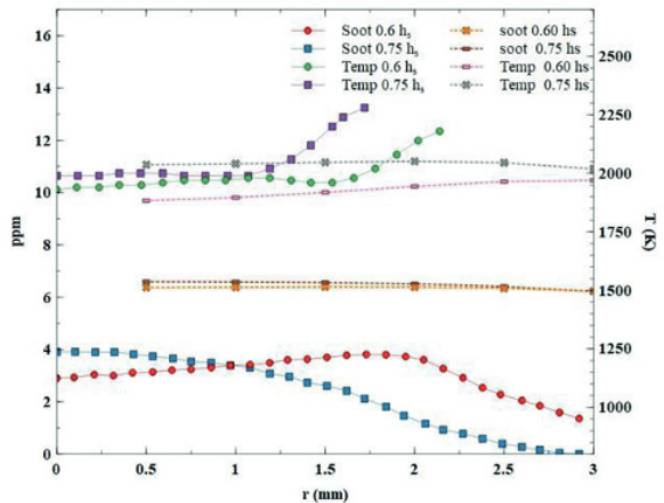


Figure 9. Comparison between numerical and experimental results for the same radius.

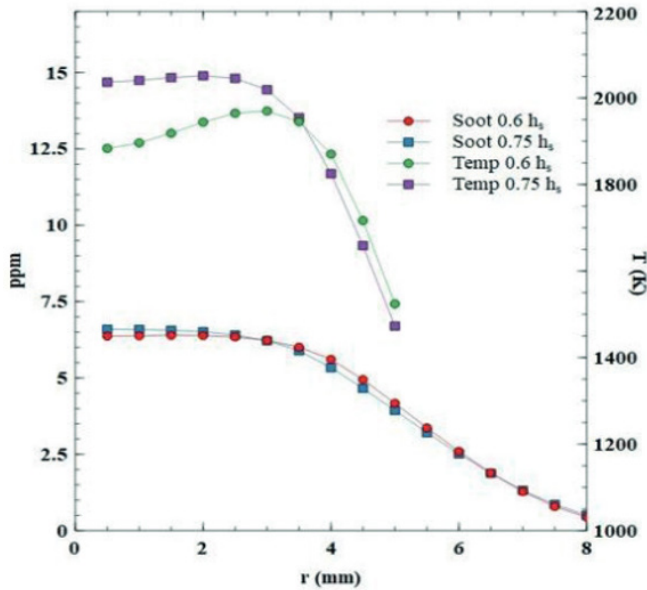


Figure 10. Soot formation and temperature.

### 3.3 LES and DNS Comparison

The simulations compare two models, LES and DNS, to predict maximum soot formation. Both models align with experimental results, but not with the distribution itself. The LES model presents lower temperatures on average, with a difference of 400K compared to DNS, as shown in Figure 11. This temperature difference is due to indeterminacy in the temperature field for LES. These two models also differ in their computational time for simulations. DNS requires more computational resources due to its method of solving equations. The differences in the results using LES may be due to the assigned mesh size, which may not collect all the necessary information of the velocity and temperature field to predict more accurately the experimental results.

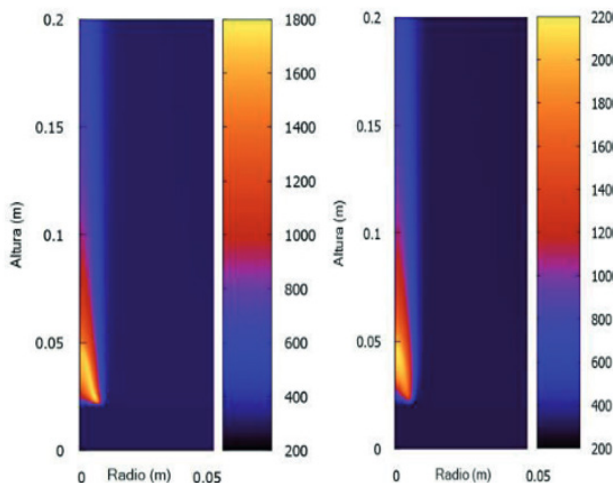


Figure 11. Comparison between LES and DNS within the simulation using mass flow per unit area.

## 4. Conclusions

An analysis of the results shows that increasing the simulation time and refining the mesh stabilizes the flame generated when using flow velocity as the calculation parameter, compared to simulations using the mass flow of gases.

The disparity between the experimental and numerical results can be attributed to the oversimplified reaction utilized in the simulations. The simulations only consider a one-step reaction instead of a more detailed reaction mechanism, which would enable a more precise prediction of the experimental results. The simulations can accurately predict soot formation and maximum temperatures at a specific oxygen percentage. Although the simulation results do not accurately produce the soot formation and temperature profiles, they do show a similar profile to that found experimentally, as demonstrated in Figures 7 and 10, but at a different radius. Among the cases studied, the simulation using the mass flow per unit area as a parameter gives a flame height that is closest to the experimental one. Conversely, the simulation using velocity as the flow definition parameter leads to an overestimation of the flame height. It is important to note that the deviation between the results of the studied cases and the experimental data cannot be attributed to the meshing procedure, i.e., the adoption of a finer mesh. This is because a finer mesh does not necessarily result in a greater number of points; instead, the temperature and soot formation distributions remain unchanged. It should be noted that in the context of Large Eddy Simulation (LES), the use of a finer mesh can actually improve the accuracy of the temperature field predictions.

## 5. Referencias

- [1] A. J. Cardona-Vargas, C. Echeverri - Uribe, J. Zap-ata-López, J. Jaramillo-Álvarez, C. Arrieta-Gón-zalez, y A. Amell-Arrieta, "Cálculo de propiedades de combustión y análisis de estabilidad de llama para el gas límite 65%CH<sub>4</sub> + 35%H<sub>2</sub>", *Rev. Ingenio*, vol. 17, n.º 1, pp. 1–8, ene. 2020. Doi: <https://doi.org/10.22463/2011642X.232>.
- [2] H. A. Yepes-Tumay y A. Cardona-Vargas, "Influence of high ethane content on natural gas ignition", *Rev. Ingenio*, vol. 16, n.º 1, pp. 36–42, ene. 2019. Doi: <https://doi.org/10.22463/2011642X.238>.
- [3] R. Henríquez, R. Demarco, J. L. Consalvi, F. Liu, and A. Fuentes, "The oxygen index on soot production in propane diffusion flames," in *Combustion Science and Technology*, May 2014, vol. 186, no. 4–5, pp. 504–517. Doi: <https://doi.org/10.1080/00102202.2014.883226>.
- [4] K. T. Kang, J. Y. Hwang, S. H. Chung, and W. Lee, "Soot zone structure and sooting limit in diffusion flames: Comparison of counterflow and co-flow flames," *Combust. Flame*, vol. 109, no. 1–2, pp. 266–281, Apr. 1997. Doi: <https://doi.org/10.1016/>

- S0010-2180(96)00163-0
- [5] Y. Zhang, H. Zhou, M. Xie, Q. Fang, and Y. Wei, "Modeling of soot formation in gas burner using reduced chemical kinetics coupled with CFD code," *Chinese J. Chem. Eng.*, vol. 18, no. 6, pp. 967–978, 2010. Doi: [https://doi.org/10.1016/S1004-9541\(09\)60155-5](https://doi.org/10.1016/S1004-9541(09)60155-5).
- [6] I. M. Kennedy, "Models of soot formation and oxidation," *Prog. Energy Combust. Sci.*, vol. 23, no. 2, pp. 95–132, Jan. 1997. Doi: [https://doi.org/10.1016/S0360-1285\(97\)00007-5](https://doi.org/10.1016/S0360-1285(97)00007-5).
- [7] K. M. Leung, R. P. Lindstedt, and W. P. Jones, "A simplified reaction mechanism for soot formation in nonpremixed flames," *Combust. Flame*, vol. 87, no. 3–4, pp. 289–305, 1991. Doi: [https://doi.org/10.1016/0010-2180\(91\)90114-Q](https://doi.org/10.1016/0010-2180(91)90114-Q).
- [8] C. C. Lee, M. V. Tran, B. T. Tan, J. B. Ooi, C. T. Chong, and G. Scribano, "A numerical study on soot formation in methane-ethanol diffusion flames," *Fuel*, vol. 328, no. July, p. 125313, 2022. Doi: <https://doi.org/10.1016/j.fuel.2022.125313>
- [9] F. Escudero, A. Fuentes, J. L. Consalvi, F. Liu, and R. Demarco, "Unified behavior of soot production and radiative heat transfer in ethylene, propane and butane axisymmetric laminar diffusion flames at different oxygen indices," *Fuel*, vol. 183, pp. 668–679, Nov. 2016. Doi: <https://doi.org/10.1016/J.FUEL.2016.06.126>.
- [10] K. McGrattan, S. Hostikka, R. McDermott, J. Floyd, and M. Vanella, "Sixth Edition Fire Dynamics Simulator User's Guide (FDS)," *Natl. Inst. Stand. Technol. Spec. Publ. 1019*, vol. Sixth Edit, p. 434, 2022. Doi: <http://dx.doi.org/10.6028/NIST.SP.1019>.
- [11] K. McGrattan, S. Hostikka, R. McDermott, J. Floyd, and M. Vanella, "Sixth Edition Fire Dynamics Simulator Technical Reference Guide Volume 1 : Mathematical Model," *Natl. Inst. Stand. Technol. NIST Spec. Publ. 1018-1*, vol. Sixth Edit, p. 207, 2022. Doi: <http://dx.doi.org/10.6028/NIST.SP.1018>.
- [12] K. B. McGrattan and G. P. Forney, "Fire dynamics simulator (version 4):," Gaithersburg, MD, 2004.
- [13] W. Yang and W. Blasiak, "Numerical simulation of properties of a LPG flame with high-temperature air," *Int. J. Therm. Sci.*, vol. 44, no. 10, pp. 973–985, Oct. 2005. Doi: <https://doi.org/10.1016/j.ijthermalsci.2005.03.001>
- [14] "ICSC 0319 - PROPANO." [Online]. Available: [http://www.ilo.org/dyn/icsc/showcard.display?p\\_version=2&p\\_card\\_id=0319&p\\_lang=es](http://www.ilo.org/dyn/icsc/showcard.display?p_version=2&p_card_id=0319&p_lang=es)